# Size-induced phase transition in $PbTiO_3$ nanocrystals: Raman scattering study

Desheng Fu
*Satellite Venture Business Laboratory, Shizuoka University, Johoku 3-5-1, Hamamatsu 432-8561, Japan; Research Institute of Electronics, Shizuoka University, Johoku 3-5-1, Hamamatsu 432-8011, Japan; and Department of Physics, Zhongshan University, Guangzhou 510275, People's Republic of China*

Hisao Suzuki
*Faculty of Engineering, Shizuoka University, Johoku 3-5-1, Hamamatsu 432-8561, Japan*

Kenji Ishikawa
*Research Institute of Electronics, Shizuoka University, Johoku 3-5-1, Hamamatsu 432-8011, Japan*
(Received 27 December 1999)

We report a Raman scattering study of $PbTiO_3$ (PT) nanocrystals prepared by a sol-gel method at a low temperature of 400 °C. The Raman spectra indicated the existence of a stable ferroelectric phase in the PT nanocrystals at room temperature. The temperature dependence of the spectrum revealed the appearance of a new phase transition in the 7-nm PT nanocrystals in the region of 166 °C. This was attributed to the phase transition between $C_{4v}$ and $C_{2v}$ point groups induced by the size reduction of the PT crystals to nanoscale. This feature is significantly different from that observed for conventional PT materials in which only the tetragonal phase is detectable below 493 °C.

## I. INTRODUCTION

Phase transitions occurring in lead titanate (PT) are of great interest subject and have been studied intensively over the last 30 years. Many studies have particularly focused on PT single crystals. The general characteristics of this ferroelectric crystal are expected to be similar to those of the prototype barium titanate (BT). Since BT has three ferroelectric phase transitions, cubic to tetragonal (120 °C), tetragonal to orthorhombic (5 °C), and orthorhombic to rhombohedral (−90 °C), for many years much work has been directed towards finding evidence for the occurrence of other phase transitions in PT in the low-temperature region. X-ray studies and dielectric measurements of PT powder samples indicated small anomalies[1–3] at temperatures close to −100 °C and −150 °C. The authors of these works suggested the possibility of an antiferroelectric transition at −100 °C in PT. Recent accurate measurements of lattice parameters and the anisotropy of optical susceptibilities of PT single crystals show that PT undergoes a phase transition at −90°C between the $C_{4v}$ and $C_{2v}$ point groups but that the lattice distortion of the $C_{2v}$ phase is extremely small (axial ratios $a/b<1.0002$ and axial angles $\beta=\gamma=90°$).[4] This small distortion evidently leads to difficulty when seeking low-temperature phase transitions in PT bulk materials, and thus most investigations have reported that only a cubic-tetragonal transition at 493 °C appears in PT bulk material.[5–7] Considered from a theoretical aspect, recent first-principle calculations[8] draw a physical picture of the origin of ferroelectricity in perovskite oxides, and demonstrate that hybridization between the $B$ cation and O is essential for ferroelectricity in $ABO_3$ perovskite ferroelectrics. In addition, the $A$ cation can modify the ground state and nature of the transition by ferroelectric distortion and hybridization with the valence state. The large strain in PT bulk materials stabilizes the tetragonal structure over the rhombohedral phase. In contrast, in BT the tetragonal strain is small and only the low-temperature rhombohedral phase is expected to be well ordered. However, these calculations also imply that other phase transitions besides the cubic to tetragonal one should occur if the ferroelectric distortion in PT materials could be tuned to a small value. The nanotechnique developed in materials science makes it possible to tune the ferroelectric distortion in PT fine crystals. Investigations by x-ray diffraction show that tetragonality ($c/a$) decreases as size is reduced to the nanometer scale for both PT and BT particles.[9–11] Thus, it is of great interest to examine the phase transition in PT nanometer particles experimentally.

The structures of the microcrystals as small as crystals of a few nanometers, usually called quantum dots, can be characterized by various techniques including x-ray diffraction (XRD), transmission electron microscopy (TEM), and Raman scattering. XRD and TEM have been widely used to study the size effects in perovskite-type ferroelectric materials, in particular for PT and BT nanocrystals. Diffraction peaks cannot be separated accurately because they broaden remarkably and overlap when particle size is reduced to the nanoscale. Thus a pseudocubic structure has been generally derived upon application of this technique to PT nanocrystals. Raman studies of metal[12,13] and semiconductor[14] nanocrystals indicate that this technique is well suited to the study of nanometric-sized systems that may show features that differ greatly from the bulk materials. Raman scattering has also been shown to be very sensitive for the detection of phase transitions in PT.[15] In the present work, Raman scattering was selected to investigate the structural phase transitions in PT nanocrystals. Some new information on phase transitions in these nanometric-sized systems has been discovered. This will be of great value for understanding the ferroelectricity in perovskite-type ferroelectric materials.

 

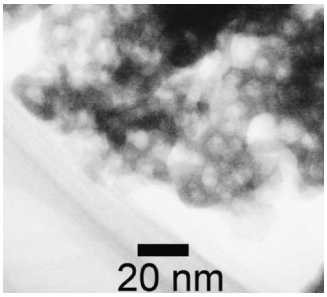


FIG. 1. TEM image of the 7-nm PT nanocrystals.

## II. EXPERIMENT

Nanocrystalline PT materials were prepared using a sol-gel method. The precursor solution of stoichiometric composition was prepared from lead acetate and titanium isoproxide using alcohol as a solvent and was refluxed to form a double alkoxide. Amorphous powders were then obtained by drying the precursor with a vacuum evaporator at room temperature. In order to control the particle size on the nanoscale, it is necessary to set the annealing temperature as low as possible. A previous study on the growth of the PT fine particles reported that crystallization can proceed at a temperature as low as 400 °C.[16] The nanoparticles used in the present study were obtained by calcination at 400 °C in air for 30 h. The average size was estimated by TEM to be about 7 nm as shown in Fig. 1.

Raman spectroscopy measurements were performed with a JOBIN YVON RAMANOR HG-2S Raman spectrometer in backscattering geometries. The 488-nm line of an argon ion laser was used as the excitation source at a power level of 30 mW. The width of both the entrance and exit slits was set at 200 $\mu$m corresponding to a spectral resolution of 1.8 $cm^{-1}$. Due to the low Raman signal level, each spectrum was the result of the addition of several scans.

The holder filled with a sample was mounted on a large metal block located in a temperature-controlled furnace constructed from ceramics with a Pyrex window. The temperature of the sample was monitored by two thermocouples inserted into the metal block close to the sample. The variation in temperature of the sample was determined to be less than $\pm 0.5$ °C during measurement. Measurements were carried out at a lower temperature than the annealing temperature in order to avoid unexpected growth of particles. The Raman spectrum at room temperature did not change after heating the sample to 361 °C.

## III. RESULTS AND DISCUSSION

The Raman spectra obtained at room temperature are illustrated in Fig. 2. It should be noted that the Rayleigh scattering extending up to 6 $cm^{-1}$ only was subtracted from the low-frequency profile for all spectra. For greatest accuracy, only the spectral profile higher than 15 $cm^{-1}$ was considered. For comparison, the figure also includes the spectra of particles with an average size of 17 nm and the amorphous powders used for obtaining the 7- and 17-nm particles. The 7-nm particles exhibited unique spectral features that were different from those of the amorphous powder and 17-nm particles. The structure of the 17-nm particles was confirmed

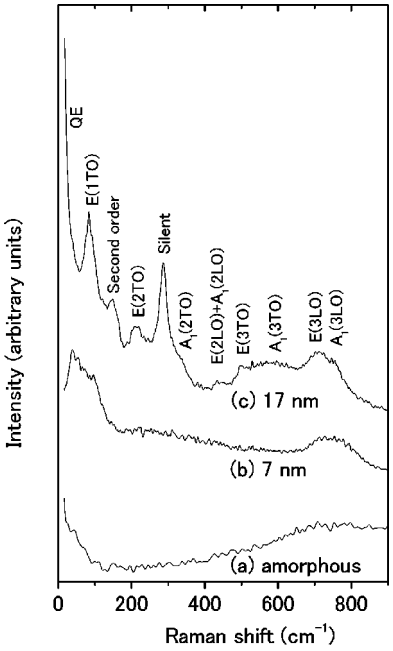


FIG. 2. Raman spectra at room temperature for the nanometric-sized PT particles. (a) Unannealed amorphous powder, (b) annealed at 400 °C for 30 h with an average size of 7 nm, (c) annealed at 400 °C for 50 h with an average size of 17 nm.

as the tetragonal phase of PT by XRD. In addition, the Raman spectrum contained all of the essential features of tetragonal polycrystalline solids prepared by conventional ceramic techniques.[17] The lowest mode is the well-known $E(1\mathrm{TO})$ soft mode of PT. The 140-$cm^{-1}$ mode used to be thought of as a second-order phonon mode.[15] The second strongest mode, assigned as $B_1+E$, is a silent mode. The other modes denoted in the figure are weak in comparison with the soft mode, and partially overlap with each other. An intense quasielastic scattering appears beside the soft $E(1\mathrm{TO})$ mode. This was usually detected even at room tem-

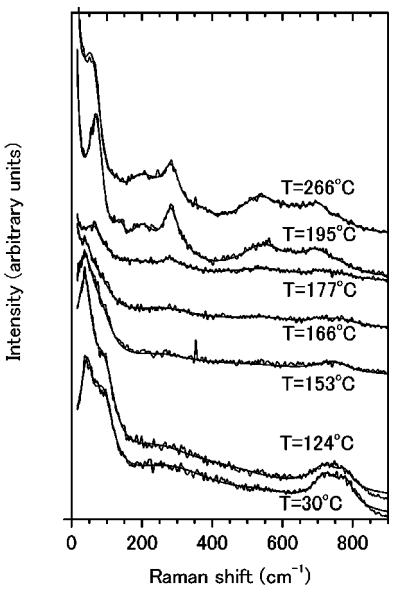


FIG. 3. Typical spectra of the 7-nm PT nanocrystals as a function of temperature. Full lines represent the fitting results using Eq. (1).

perature in the low dimensional systems of tetragonal PT,[18,19] while it was observable only in the vicinity of the Curie point for the bulk by careful measurement.[20] This quasielastic scattering was attributed to a Debye relaxation mode derived from an order-disorder process.[20] The spectrum of the amorphous powder displays no distinct Raman scattering peak except for a broad band. Figure 2 clearly shows that the 7-nm particles have a quite different structure. This structure is neither the amorphous nor tetragonal phase of PT. Two partially overlapping intense peaks can be seen in the low-frequency and the high-frequency profile, while only a broad band is present in the middle region.

To study the phase of the 7-nm particles at room temperature, Raman spectra were then recorded as a function of temperature. Figure 3 illustrates the Raman spectra at several typical temperatures. As the temperature increases, the spectral profile above $200\,\mathrm{cm}^{-1}$ varies slightly, in contrast the low-frequency profile clearly changes. The two modes are easily resolved. The intensity of the lowest mode at about $50\,\mathrm{cm}^{-1}$ (mode 1) is much larger than that of its neighbor around $100\,\mathrm{cm}^{-1}$ (mode 2). The spectra become quite weak after further heating. In the vicinity of 166 °C, these two modes appear to degenerate, and the quasielastic scattering becomes visible. It is evident that there is a phase transition around this temperature ($T_c^{\mathrm{O\text{-}T}}$) above which another phase with essentially different features is formed. This high-temperature phase can be unambiguously attributed to the tetragonal structure of PT by comparison with the spectrum of the 17-nm PT particles that have a tetragonal phase at room temperature as shown in Fig. 2(c).

In order to understand the features of the Raman spectra as a function of temperature, we fitted the observed spectra with a spectral response, which is the simple sum of damped harmonic oscillators and a Debye relaxation mode (the quasielastic scattering):[20]

$$I(\omega)=\left(\frac{1}{e^{h\omega/kT}-1}+1\right)\begin{cases}\left(\displaystyle\sum_i \frac{2\Gamma_i F_i \omega\omega_i^3}{(\omega_i^2-\omega^2)^2+4\Gamma_i^2\omega_i^2\omega^2}\right) & \text{for } T<166\,^\circ\mathrm{C}\\ \left(\dfrac{F_r\omega\gamma_r}{\omega^2+\gamma_r^2}+\displaystyle\sum_i \frac{2\Gamma_i F_i \omega\omega_i^3}{(\omega_i^2-\omega^2)^2+4\Gamma_i^2\omega_i^2\omega^2}\right) & \text{for } T\geqslant 166\,^\circ\mathrm{C},\end{cases} \tag{1}$$

where the former term is the Bose-Einstein factor, $\omega_i$, $\Gamma_i$, and $F_i$ are the mode frequency, damping factor, and oscillator strength, $\gamma_r$ and $F_r$ are the inverse relaxation time and strength associated with the relaxation mode. Because of the weak intensity, the quasielastic scattering at temperatures lower than $T_c^{\mathrm{O\text{-}T}}$ was not considered in the fitting procedures. Figure 4 shows typical results for fits at two temperatures located above and below $T_c^{\mathrm{O\text{-}T}}$ so that all modes are seen separately. It is obvious that the fits are quite satisfactory.

In Fig. 5, the observed mode frequencies are presented as a function of temperature. The modes in the high-temperature tetragonal phase can be easily identified by comparison with those in the 17-nm PT particles spectrum, Fig. 2(c). Special attention should be drawn to the lowest mode, the $E(1\mathrm{TO})$ mode. This mode dominates the dielectric be-

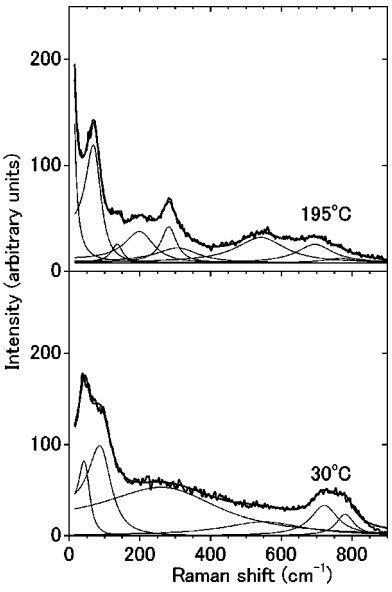


FIG. 4. Typical results of fits using Eq. (1) so that all modes are seen separately. Full lines represent the fitting results.

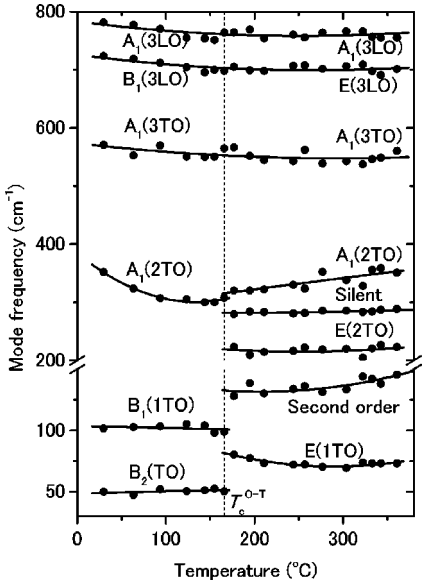


FIG. 5. Temperature dependence of the mode frequencies in 7-nm PT nanocrystals. Full lines represent least-squares fits using polynomials with up to cubic terms in $T$ to guide the eye.

havior of PT, and is related to the ferroelectric phase transition[21] and is usually called a soft mode. It is shifted to low frequency in comparison with those ($89\,\mathrm{cm}^{-1}$ at room temperature) in bulk materials, implying a lowering of the force constant in the nanocrystals. This feature was observed for the ultrafine PT particles, leading to the decrease of the phase transition temperature between the tetragonal and cubic phase.[18] Although we have not observed the tetragonal-cubic phase transition in the present sample due to the limitation of possible size increase at higher temperature, the measured spectrum at 361 °C is so weak that it can be expected that the scattering peaks will disappear and the phase transition should appear in the vicinity of this temperature. The soft mode first softens as the temperature increases. However, there seems to be no further softening as the temperature further increases. The exact reason why the PT nanocrystals as well as thin films[19] exhibit such behavior is unclear at present. In Fig. 5, one can clearly see again that the most intense double $E(1\mathrm{TO})$ mode is split into two modes at $T_c^{\mathrm{O\text{-}T}}$. Figure 6 shows the temperature dependence of the damping factors of these low-frequency modes. The damping factors of the two modes in the low-temperature phase fall within the underdamping limit,[22] while that of the $E(1\mathrm{TO})$ soft mode tends to become overdamping as the temperature increases. It should be noted that the soft mode damping factor in PT nanocrystals is significantly larger than that in the single crystals.[15,21] A discontinuity of the damping factors around 166 °C can also be seen in Fig. 6, indicating again that the modes above and below this temperature belong to different structures.

We now discuss the origin of the low-temperature phase. Impurities that might be included in the samples are organic compounds in the precursor. Since the samples have been annealed at 400 °C for 30 h, it is unlikely that the organic compounds still reside in the samples. It can also be seen from Fig. 2(a) that the organic compounds have no influence on the Raman spectra. The pyrochlore phase that might develop during annealing can be excluded by the fact that the pyrochlore-tetragonal phase transition is not reversible while Raman measurement at room temperature after heating to 361 °C proves that the observed phase transition in the sample is reversible. Raman measurements of metal[12,13] and semiconductor[14] nanocrystals revealed the occurrence of confined acoustic phonons in the low-frequency region. This can be used to explain the appearance of the lowest mode (mode 1) at room temperature, but mode 2 cannot be attributed to the $E(1\mathrm{TO})$ soft mode because of the discontinuity in mode frequency shown in Fig. 5.

The stable phase at room temperature can therefore be regarded as a new crystalline state of PT materials. The phase transition at $T_c^{\mathrm{O\text{-}T}}$ is due to the symmetry change of the unit cell of the PT nanocrystals. It has been reported that a lattice relaxation is present near the surface of PT within two layers,[10] and thus the 7-nm PT nanocrystals consisted of about 20% of atoms that reside in the surface region.[23] The large fraction of the surface layer will then strongly influence the structures of the PT nanocrystals. Investigation of the lattice parameter shows that the tetragonality $c/a$ reduces to nearly unity for PT particles for sizes less than 10 nm at room temperature.[9] Thus, the energy difference between the cubic and tetragonal structure in the PT nanocrystals should

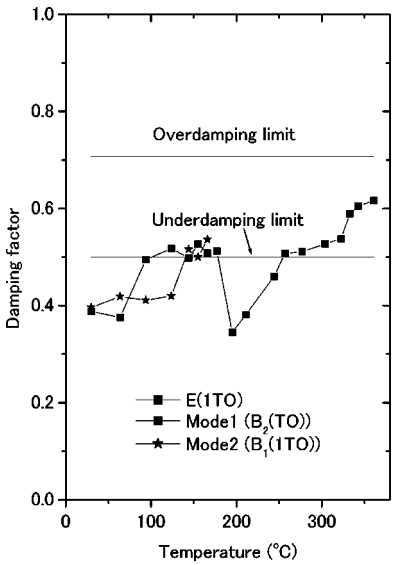


FIG. 6. Damping factor as a function of temperature for the low-frequency modes in 7-nm PT nanocrystals. The curves are to guide the eye.

be significantly less than that in the bulk materials, and the other low-temperature phase is expected to be well ordered in a similar way to BT.[8] It then follows that the PT nanocrystal system is orthorhombic at room temperature. On the basis of the work of Kobayashi *et al.* on single crystals,[4] it would be reasonable to assign the point group of the low-temperature phase of the PT nanocrystals as $C_{2v}$. The theoretical study shows that the $E(1\mathrm{TO})$ soft mode corresponds to the vibration of both Ti and O ions against Pb ions along the *a* or *b* axis.[24] As the phase transition between $C_{4v}$ and $C_{2v}$ occurs at $T_c^{\mathrm{O\text{-}T}}$ in the PT nanocrystals, the double mode $E(1\mathrm{TO})$ will disappear and two split modes should appear in the low-symmetry systems due to the lattice distortion along the *a* and *b* axis. It is clear now that mode 1 and mode 2 can be assigned as $B_2(\mathrm{TO})$ and $B_1(1\mathrm{TO})$ modes, respectively, by comparison with results from the isomorphic compound BT (Ref. 25) and $KNbO_3$.[26] The other modes in the orthorhombic phase are then identified in the same manner as shown in Fig. 5.

## IV. CONCLUSION

Raman scatterings in PT nanocrystals proved the existence of a phase transition around 166 °C above which the tetragonal phase is developed and below which the orthorhombic phase is stable. The transition temperature is about 260 °C higher than that reported in single crystals.[4] The lowest two split modes have been observed in the low-temperature phase and assigned as the $B_2(\mathrm{TO})$ and $B_1(1\mathrm{TO})$ modes of the orthorhombic phase. These interpretations are supported by recent first-principle investigation on the origin of perovskite-type ferroelectricity[8] and accurate measurements of lattice parameters[4] in this material. All these results are favorable for understanding of the origin of ferroelectricity and size effects in perovskite-type ferroelectrics. Further research on these nanophase materials is clearly necessary.

**ACKNOWLEDGMENTS**

We wish to thank Dr. S. Tsunekawa of Tohoku University for help in preparing the TEM image. Part of this work was supported by a Grant-in-Aid for General Scientific Research (B) from the Ministry of Education, Science and Culture of Japan.

[1] J. Kobayashi and R. Ueda, Phys. Rev. **99**, 1900 (1955).
[2] J. Kobayashi, S. Okamoto, and R. Ueda, Phys. Rev. **103**, 830 (1956).
[3] S. Ikegami, I. Ueda, and T. Miyazawa, J. Phys. Soc. Jpn. **26**, 1324 (1969).
[4] J. Kobayashi, Y. Uesu, and Y. Sakemi, Phys. Rev. B **28**, 3866 (1983).
[5] J. P. Remeika and A. M. Glass, Mater. Res. Bull. **5**, 37 (1970).
[6] A. M. Glazer and S. A. Mabud, Acta Crystallogr., Sect. B: Struct. Crystallogr. Cryst. Chem. **B34**, 1065 (1978).
[7] S. A. Mabud and A. M. Glazer, J. Appl. Crystallogr. **12**, 49 (1979).
[8] R. E. Cohen, Nature (London) **358**, 136 (1992).
[9] K. Ishikawa and K. Nagareda, J. Korean Phys. Soc. **32**, S56 (1998).
[10] K. Ishikawa and T. Uemori, Phys. Rev. B **60**, 11 841 (1999).
[11] S. Chattopadhyay, P. Ayyub, V. R. Palkar, and M. Multani, Phys. Rev. B **52**, 13 177 (1995).
[12] E. Haro-Poniatowski, M. Jouanne, J. F. Morhange, M. Kanehisa, R. Serna, and C. N. Afonso, Phys. Rev. B **60**, 10 080 (1999).
[13] M. Fujii, T. Nagareda, S. Hayashi, and K. Yamamoto, Phys. Rev. B **44**, 6243 (1991).
[14] M. Fujii, Y. Kanzawa, S. Hayashi, and K. Yamamoto, Phys. Rev. B **54**, R8373 (1996).
[15] G. Burns and B. A. Scott, Phys. Rev. Lett. **25**, 167 (1970).
[16] K. Ishikawa, N. Okada, K. Takada, T. Nomura, M. Hagino, and K. Toyoda, Jpn. J. Appl. Phys., Part 1 **33**, 5412 (1994).
[17] G. Burns and B. A. Scott, Phys. Rev. Lett. **25**, 1191 (1970).
[18] K. Ishikawa, K. Yoshikawa, and N. Okada, Phys. Rev. B **37**, 5852 (1988).
[19] D. S. Fu, H. Iwazaki, H. Suzuki, and K. Ishikawa, J. Phys.: Condens. Matter **12**, 1 (2000).
[20] M. D. Fontana, H. Idrissi, and K. Wojcik, Europhys. Lett. **11**, 419 (1990).
[21] G. Burns and B. A. Scott, Phys. Rev. B **7**, 3088 (1973).
[22] M. DiDomenico, Jr., S. H. Wemple, S. P. S. Porto, and R. P. Bauman, Phys. Rev. **174**, 522 (1968).
[23] R. W. Siegel, Annu. Rev. Mater. Sci. **21**, 559 (1991).
[24] J. D. Freire and R. S. Katiyar, Phys. Rev. B **37**, 2074 (1988).
[25] Y. Luspin, J. L. Servoin, and F. Gervais, J. Phys. C **13**, 3761 (1980).
[26] M. D. Fontana, G. Métrat, J. L. Servion, and F. Gervais, J. Phys. C **16**, 483 (1984).